

# **MODELLING OF ISOTHERMAL FERRITE FORMATION USING AN ANALYTICAL TREATMENT OF SOFT IMPINGEMENT IN 0.37C – 1.45Mn – 0.11V MICROALLOYED STEEL**

C. García de Andrés<sup>1</sup>, C. Capdevila<sup>1</sup>, F.G. Caballero<sup>1,2</sup> and H.K.D.H. Bhadeshia<sup>2</sup>

<sup>1</sup> Department of Physical Metallurgy

Centro Nacional de Investigaciones Metalúrgicas (CENIM)

Consejo Superior de Investigaciones Científicas (CSIC)

Avda. Gregorio del Amo, 8. 28040 Madrid, Spain

<sup>2</sup> Department of Materials Science and Metallurgy

University of Cambridge

Pembroke Street, Cambridge CB2 3QZ, UK

## **Introduction**

Allotriomorphic ferrite is usually the first phase to form from austenite at temperatures below  $Ae_3$ . The ferrite as it grows modifies the composition of the residual austenite and the reaction rate is affected by this solute partitioning. Ferrite allotriomorphs nucleate at the prior austenite grain boundaries (1-3) and grow both along the boundaries and into the austenite grains.

A simple model for the growth of grain boundary allotriomorphs involves the one-dimensional movement of a planar  $a/g$  interface. The growth rate of allotriomorphs is controlled by carbon diffusion in the austenite located ahead of the interface, with local equilibrium in the phases in contact at the interface (4). The growth of allotriomorphic ferrite takes place mainly in two stages. The first involves parabolic growth from opposing sides of an austenite grain, a process which can be readily treated (5-7). The duration of this stage will depend on the time needed for the carbon diffusion fields from different allotriomorphs to significantly overlap. This overlap is known as soft impingement and may occur between allotriomorphs placed on the same or different faces, edges and corners of the austenite grain boundary (8). During soft impingement, the austenite is considered to have a finite extent beyond the  $a/g$  interface. Therefore, the carbon concentration in the centre of the austenite grain is given by balancing the amount of carbon enrichment of the austenite against the corresponding depletion of the ferrite (4,8).

The present paper is concerned with a theoretical and experimental description of the growth kinetics of allotriomorphic ferrite in a medium carbon microalloyed steel. Moreover, the effect of the soft impingement on the growth kinetics of allotriomorphic ferrite is treated using an analytical treatment based on work by Gilmour et al. (9). We have neglected nucleation in the theoretical interpretation, because as will be seen later, the incubation time is very short compared with that required to achieve complete transformation.

## **Materials and Experimental Procedure**

The chemical composition of the steel studied is presented in Table 1. The material was supplied in the form of 50 mm square bars, obtained by conventional casting to a square ingot (2500 kg) and hot rolling to bar. Cylindrical dilatometric test pieces of 2 mm diameter and 12 mm length were machined parallel to the rolling direction of the bar. Heat treatments were carried out in the heating and cooling devices of a high resolution dilatometer DT 1000 Adamel-Lhomargy described elsewhere (10). The heating device consists of a very low thermal inertia radiation furnace. The power radiated by two tungsten filament lamps is focussed on the specimen by means of a bi-elliptical reflector. The temperature is measured with a 0.1 mm diameter Chromel – Alumel (Type K) thermocouple welded to the specimen. Cooling is carried out by blowing a jet of helium gas directly onto the specimen surface. The helium flow rate during cooling is controlled by a proportional servovalve. These devices ensure an excellent efficiency in controlling the temperature and holding time of isothermal treatments, and fast cooling in quenching processes. Specimens were austenitized at 1273 K and 1523 K for 1 min and subsequently isothermally transformed at 973 K during different times. In order to freeze the microstructure at that temperature, specimens were quenched under helium gas flow at a cooling rate of 200 K/s. Specimens were polished in the usual way for metallographic examination. Nital - 2pct etching solution was used to reveal the ferrite microstructure by optical microscopy. The prior austenite grain size (PAGS) measurements were made on micrographs. The average grain size was estimated by counting the

number of grains intercepted by one or more straight lines long enough to yield, in total, at least fifty intercepts. The effects of a moderately non-equiaxial structure may be eliminated by counting the intersections of lines in four or more orientations covering all the observation fields with an approximately equal weight (11). Table 2 shows the average PAGS in microns. Moreover, the volume fraction of allotriomorphic ferrite ( $V_a$ ) was estimated statistically by a systematic manual point counting procedure (11). A grid superimposed on the microstructure provides, after a suitable number of placements, an unbiased statistical estimation of the  $V_a$ .

TABLE 1  
Chemical composition (wt - %)

C	Si	Mn	Cr	Al	Ti	V	Cu	Mo
0.37	0.56	1.45	0.04	0.024	0.015	0.11	0.14	0.025

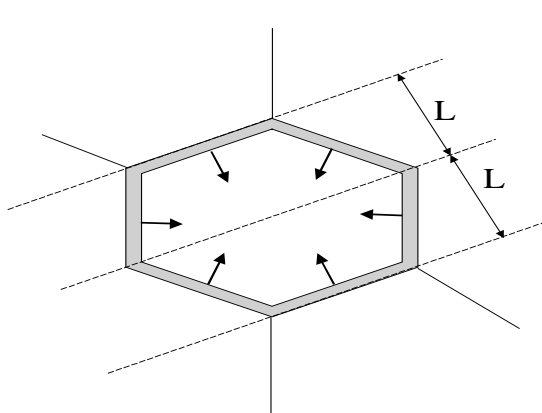
TABLE 2  
Prior austenite grain size

Tg(K)	PAGS (mm)
1523	76
1273	11

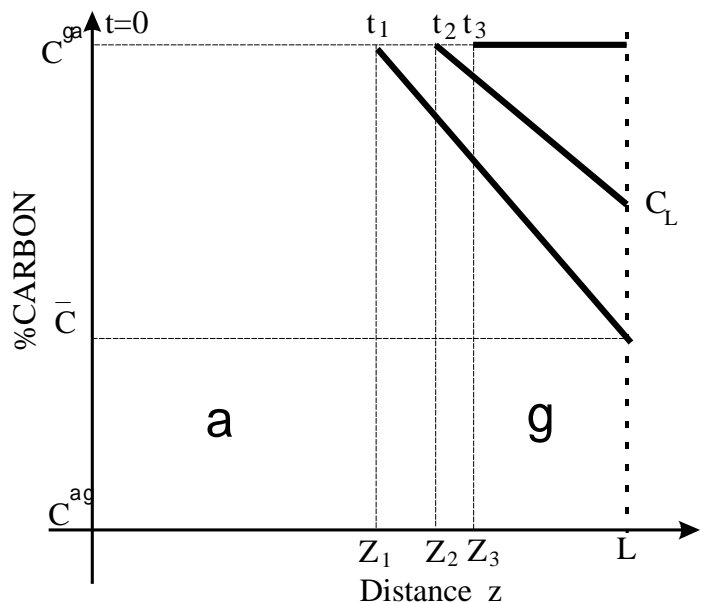
Tg = Austenitising temperature

### Results and Discussion

The following calculations deal with the one-dimensional growth of planar grain boundary allotriomorphs from opposite sides of an austenite grain as illustrated schematically in Fig. 1(a). This process may be considered in two stages. The first one involves a parabolic growth from both sides of the grain according to the assumption that austenite has a semi-infinite extent with constant boundary conditions. In this stage, the carbon concentration in austenite far from the a/g interface remains the same as the overall carbon content of the steel. During the second stage, overlapping of carbon diffusion gradients of allotriomorphs growing from opposite sides of a grain occurs, and the growth rate considerably decreases. This effect is known as soft impingement. Figure 1(b) shows a scheme of the carbon concentration profiles in austenite during the soft impingement stage. In this model, it is assumed that a/g interface moves in  $z$  direction normal to the interface plane, and austenite is considered to have a finite size  $L$  in that direction. The position of the interface at any time  $t$  is defined by  $z = Z$ , being  $Z = 0$  at  $t = 0$ . In this initial state, the carbon concentration in the austenite is uniform and corresponds to the overall carbon composition ( $\bar{C}$ ). The position of the interface at the onset of soft impingement is defined by  $z = Z_1$  and  $t = t_1$ . At that moment, carbon concentration rises at every point in the austenite located ahead of the interface. Therefore, the concentration of carbon in the centre of the austenite grain increases from  $\bar{C}$  to  $C_L$ . Finally, when  $z = Z_3$  and  $t = t_3$ , the carbon content in austenite is uniform and equal to that of austenite in the a/g interface ( $C_L = C^{ag}$ ). The composition at the interface were fixed under paraequilibrium conditions according to reference 4.



(a)



(b)

Figure 1. Diagram illustrating the soft-impingement process: (a) Schematic representation of the growth of grain boundary allotriomorphs, (b) carbon concentration profile for the calculation of impingement time.

Assuming that allotriomorphs grow on austenite grain boundaries without interfering with each other, the half-thickness of the allotriomorphs may be calculated under parabolic growth conditions according to the following expression:

$$Z = a_I t^{1/2} \quad [1]$$

where  $Z$  is the half-thickness of the allotriomorphs,  $a_I$  is the one-dimensional parabolic growth rate constant and  $t$  is the growth time. The value of  $a_I$  can be obtained by numerical solution from the equation,

$$a_I e^{\frac{a_I^2}{4D}} \operatorname{erfc} \frac{a_I}{2\sqrt{D}} = \frac{C^g - \bar{C}}{C^g - C^{ag}} \quad [2]$$

where  $D$  is the diffusivity of carbon in austenite,  $\bar{C}$  is the overall carbon content,  $C^g$  is the carbon content of austenite in equilibrium with ferrite,  $C^{ag}$  is the carbon content of ferrite in equilibrium with austenite (4, 12).

At the onset of the soft impingement when the position of the interface is  $z = Z_I$ , the carbon enrichment of the austenite is equal to the amount of carbon removed from the ferrite. The value of  $C^{ag}$  is negligibly small. Therefore, according to Fig. 1(b), the mass balance can be given by (9),

$$\frac{1}{2} (C^g - \bar{C})(L - Z_I) = \bar{C}Z_I \quad [3]$$

where  $L$  is the semi-extent of the austenite grain. This balance allows one to calculate the position of the interface  $Z_I$ ,

$$Z_I = \frac{L(C^g - \bar{C})}{(C^g + \bar{C})} \quad [4]$$

Likewise, the position of the interface  $Z_3$  when the carbon activity becomes uniform is calculated using the appropriate mass balance expressed as follows:

$$Z_3 \bar{C} = (L - Z_3)(C^g - \bar{C}) \quad [5]$$

$$Z_3 = L - \frac{\bar{C}}{C^g} \quad [6]$$

On the other hand, the carbon concentration in the centre of the austenite grain ( $C_L$ ) can be calculated also by balancing the amount of carbon enrichment of austenite against the carbon depletion in the ferrite at an intermediate position  $Z_2$  (Fig. 1(b)) during the soft impingement process ( $Z_I < Z_2 < Z_3$ ),

$$\bar{C}Z_2 = (L - Z_2) \times \frac{[(C^g - \bar{C}) + (C_L - \bar{C})]}{2} \quad [7]$$

$$C_L = \frac{2L\bar{C} - C^g \times (L - Z_2)}{L - Z_2} \quad [8]$$

The instantaneous interfacial carbon mass balance is described as follows:

$$C^g \frac{dZ}{dt} = -D \frac{dC}{dz} \quad [9]$$

where  $\frac{dC}{dz}$  represents the gradient of carbon ahead of the interface. Figure 1(b) shows that, in position  $Z=Z_2$ , this gradient can be expressed by,

$$\frac{dC}{dz} = -\frac{C^g - C_L}{L - Z_2} \quad [10]$$

Finally, combining Eqs. [8], [9], and [10] the following differential equation is obtained:

$$\frac{dZ}{dt} = \frac{2D(Z_3 - Z_2)}{(L - Z_2)^2} \quad [11]$$

This velocity expression may then be integrated to yield the time as a function of the interface position. Thus, the expression of time for  $t=t_2$  ( $Z=Z_2$ ) is given by,

$$t_2 = \frac{1}{2D} \left[ \frac{1}{2} [Z_1^2 - Z_2^2] + [2K + Z_3] \times [Z_2 - Z_1] - K^2 \ln \frac{\hat{e}^{Z_3} - Z_2 \dot{u}}{\hat{e}^{Z_3} - Z_1 \dot{u}} \right] \quad [12]$$

with  $K = L \frac{\bar{C}}{C^g}$ .

The equilibrium carbon concentration in the interface  $C^g$  is evaluated using a quasi-chemical solid solution model (13-15). The effect of alloying elements is included in the calculations via the free energy terms according to Zener (16). Moreover, the carbon diffusivity in austenite is calculated using the Siller and McLellan's method (17), which considers the nearest neighbour intersections and the effect of substitutional solutes.

Figure 2 shows the influence of the PAGS on the growth kinetics of allotiomorphic ferrite calculated in this work for this steel. This figure suggests that the rate of allotiomorphic ferrite transformation decreases as the PAGS increases, which is consistent with previous works (18-20). On the other hand, as PAGS increases, the evolution of the carbon enrichment in the centre of the austenite grain with the time is slower as is shown in Fig. 3.

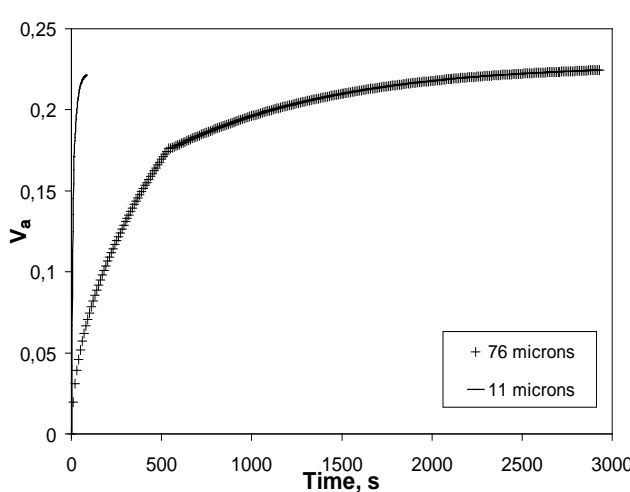


Figure 2. Influence of the PAGS in the  $V_a$  evolution.

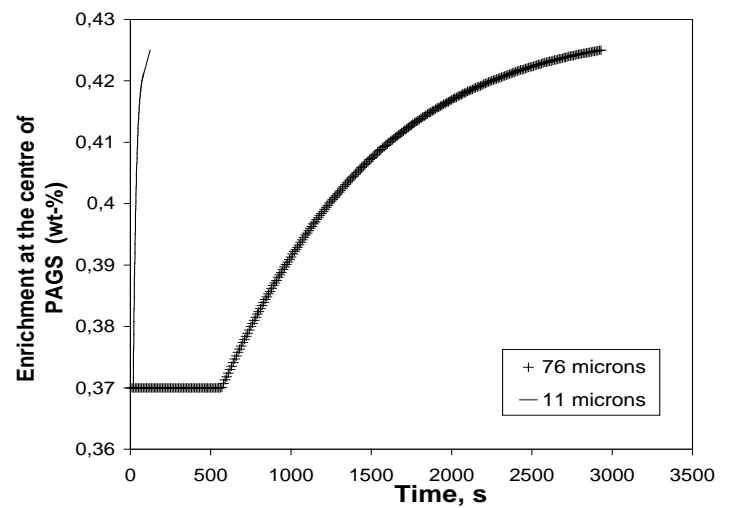


Figure 3. Influence of PAGS on the carbon enrichment in the centre of austenite grain.

A comparison of the calculated and experimental  $V_a$  is shown in Fig. 4. One can conclude from this figure that a reasonable overall level of agreement between experiment and theory exists.

Figure 5 shows the calculated and measured  $V_a$  under parabolic and soft impingement growth conditions for both PAGSs. This figure suggests that care needs to be taken with the assumption of non – infinite austenite grain extent and the modelling of allotriomorphic ferrite transformation under parabolic growth conditions in medium carbon microalloyed steels. It can be concluded that the soft impingement effect should be considered in the study of allotriomorphic ferrite growth kinetics of this steel.

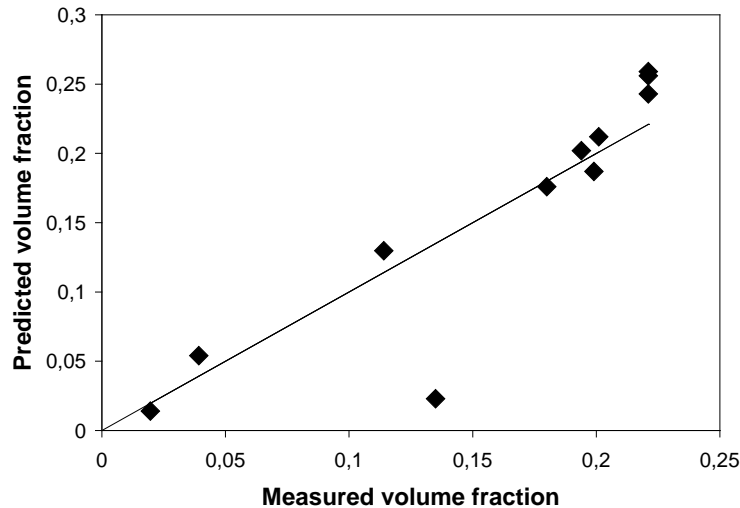


Figure 4. A comparison of the calculated volume fraction vs experimental data.

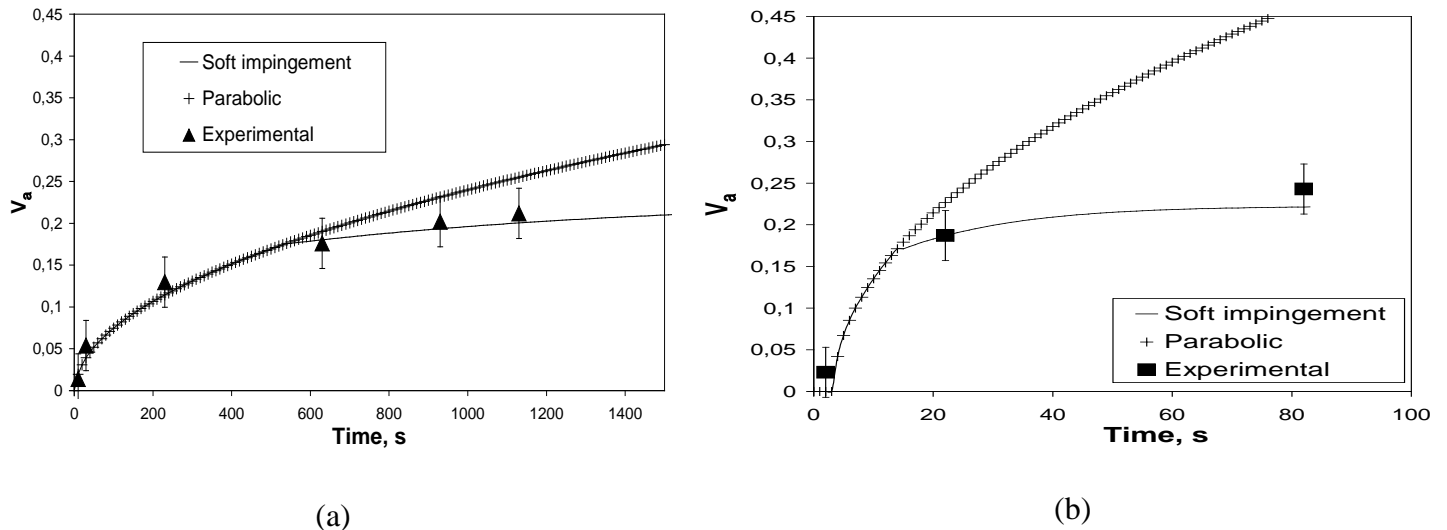


Figure 5.- Comparison between calculated and measured  $V_a$  under parabolic and impingement considerations. (a) PAGS=76 mm, (b) PAGS=11mm.

### Conclusions:

1. The assumption of constant boundary conditions is not valid for real systems where the austenite grain is finite in size, since the diffusion fields of particles growing from different points must eventually interfere.
2. It has been demonstrated that the Gilmour et al. analysis gives a very good representation of the progress of transformation in 0.37C – 1.45Mn – 0.11V microalloyed steel.

### **Acknowledgements**

CENIM's authors acknowledge financial support from the Spanish Comisión Interministerial de Ciencia y Tecnología (CICYT) (project-PETRI 95-0089-OP). GSB Acero S.A and CEIT are thanked for providing the steel and their collaboration in this project.

### **References**

1. R.F. Mehl, C.S. Barrett, and D.W. Smith, AIME Trans., 105, 215, (1933).
2. G.R. Purdy, D.H. Weichert, and J.S. Kirkaldy, AIME Trans., 230, 1025, (1964).
3. C.A. Dube, H.I. Aaronson, and R.F. Mehl, Revue de Metallurgie, 3, 201, (1958).
4. H.K.D.H. Bhadeshia, Progress in Materials Science, 29, 321, (1985).
5. J.R. Bradley and H.I. Aaronson, Metall. Trans. A, 12A, 1729, (1981).
6. S.J. Jones and H.K.D.H. Bhadeshia, Acta mater., 45, 2911, (1997).
7. S.J. Jones and H.K.D.H. Bhadeshia, Metall. and Mat. Trans., 28A, 2005, (1997).
8. C.Capdevila, C.Garcia de Andres, and H.K.D.H Bhadeshia, Materials Algorithms Project (MAP) contribution, URL: <http://www.msm.cam.ac.uk/map/steel/programs/ferr-b.html>
9. J.B. Gilmour, G.R. Purdy, and J.S. Kirkaldy, Metall. Trans., 3, 3213, (1972).
10. C. García de Andrés, G. Caruana, and L.F. Alvarez, Mater. Sci. Eng., A241, 211, (1998).
11. G.F. Vander Voort, 'Metallography. Principles and Practice', p. 427, McGraw-Hill Book Company, New York, (1984).
12. J.W. Christian, 'Theory of Transformations in Metals and Alloys', Pergamon Press, Oxford, (1965).
13. H.I. Aaronson, H.A. Domian and G.M. Pound, Trans. Metall. Soc. of AIME, 236, 753, (1966).
14. H.I. Aaronson, H.A. Domian and G.M. Pound, Trans. Metall. Soc. of AIME, 236, 768, (1966).
15. G.J. Shiflet, J.R. Bradley and H.I. Aaronson, Metall. Trans. A, 9, 999, (1978).
16. C.Zener, Trans. AIME, 203, 619, (1955).
17. R.H.Siller and R.B.McLellan,TMS-AIME, 245, 697, (1969).
18. W.A. Johnson and F.Mehl, AIME Trans., 135, 416, (1939)
19. J. Bardford and W.S. Owen, J. Iron Steel Institute, 197, 146, (1961).
20. A.K. Sinha, 'Ferrous Physical Metallurgy', p. 379, Butterworths, Boston, USA, (1989).